



EFFECT OF SURFACTANT TYPE AND AMOUNT ON THE THERMOCHROMIC PROPERTIES OF POLYDIACETYLENE

Hiba Imad Abdulkareem¹, Auda Jabbar Braihi², and Ali Salah Hasan³

¹ Polymer and Petrochemical Industries Dep./ College of Materials Engineering/
University of Babylon, Hilla, Iraq, Email; heba.mahdi@uobabylon.edu.iq

² Polymer and Petrochemical Industries Dep./ College of Materials Engineering/
University of Babylon, Hilla, Iraq, Email; audajabbar@gmail.com

³ Polymer and Petrochemical Industries Dep./ College of Materials Engineering/
University of Babylon, Hilla, Iraq, Email; mat.ali.salah@uobabylon.edu.iq

<https://doi.org/10.30572/2018/KJE/160427>

ABSTRACT

Herein we report a simple way to improve the thermochromic behavior of polydiacetylene (PCDA) by the incorporation of surfactants. modified by the addition of anionic (SDS), cationic (CTBA) and nonionic (Triton X-100) surfactants in different ratios. Polymerization was performed at room temperature by UV irradiation. We evaluated the effect of surfactant type, concentration, and temperature (25°C, 36°C, and 40°C) on thermochromism. Ideal color transitions (from blue to red at less than 40°C) were done with 0.012g SDS, 0.015g CTBA, and 1ml Triton X-100. SDS-modified PCDA was identified for textiles by CIE-Lab* results, whereas CTBA and Triton-X-100 modified PCDA for as safety indicators and smart packaging applications. Results of particle size analysis shows that SDS form the largest particle sizes with the PCDA polymer, where its D50 is 566.9 μm compared with 1.153 μm and 4. 671 μm for CTBA and Triton respectively. Using DFT calculations, it is determined that there is an increase of energy when adding a surfactant and that electronic properties of PCDA are altered with it, where it shows a decrease in energy gap, which suggests potential uses in thermoelectric materials development, sensors and in measuring temperature.

KEYWORDS

Thermochromism, Surfactant, density functional theory (DFT), polydiacetylenes, UV irradiation, CIE-Lab.



1. INTRODUCTION

Thermochromism, a reversible or irreversible change of color with temperature (Crosby, P.H. et al., 2022). Polydiacetylene (PDAs) is a significant thermochromic material and has been extensively investigated as a sensor material owing to its unique optical characteristics (Hossain, S. et al., 2022). One method for polymerization is UV initiation at a given wavelength (Hossain, M.I. et al., 2022). PDAs is polymer consists of the polymerization of monomer 10,12-pentacosadiynoic acid (PCDA). PDAs exhibits limited temperature sensitivity and usually demands elevated heat treatment for switching coloration, thus motivating the investigation of tuning the properties of PDAs, notably with surfactant inclusion. Surfactants are amphiphilic molecules with hydrophilic and hydrophobic groups that alter polymer properties (Yadav, S.N. et al., 2022). Surfactants control the surface microstructure and the thermochromic efficiency with polymer templates as well (Wang et al., 2022). The role of surfactants is critical in determining the geometrical and digital functions of thermochromic materials, in particular polydiacetylene (PDA)-based totally systems. They contact on microstructure, balance, and thermochromic behavior by means of influencing microcapsule morphology, size, and distribution, and as a result, change optical homes. Microencapsulation shells are laid low with surfactants which includes ctramonium bromide (CTAB), sodium dodecyl sulphonate (SDS), and hexadecanol, which play a critical position in emulsion stabilization, which is critical for the formation of microcapsules with desired length and morphology (Hakami, A. et al., 2022). Surfactants adjust the molecular environment in an electronic way where the maximum probably digital transitions showcase absorption spectrum shifts, which have an effect on the colorimetric response. Furthermore, they enhance the steadiness and reversibility of the thermochromic response (Kim, I. et al., 2018). The particle length evaluation is crucial for surfactant-changed PDAs polymers which points out the significance of surfactant attention and sort on particle size and stability. Increasing surfactant awareness will lower the particle size via reducing interfacial anxiety, at the same time as the great stabilization takes place at across the crucial micelle concentration (CMC) (Stanfield, M.K. et al., 2024). The chemistry of surfactants also affects particle formation; nonionic surfactants consisting of Triton X-100 produce plenty smaller particles than anionic surfactants which includes SDS (Banjar, M.F. et al., 2023). Other elements consisting of the polymer awareness also have an effect on the particle size, as with better polymer attention it increases the viscosity and thus large debris (Ibadat, N. et al., 2021). Process parameters, such as sonication time and shear rates additionally impact particle stability and length distribution. It became charming to be aware the specific interactions of surfactants and polymers and the way this may affect the final particle

characteristics (Zhang, L. et al., 2023). The thermochromism of polymers, as an instance, can be described and expected correctly using the powerful Density Functional Theory (DFT). DFT affords insight into electronic shape, which illustrates how the polymer digital states are impacted via temperature (Gupta, S. et al., 2020). For instance, DFT is used to take a look at polymer-nanoparticle interactions in polymers to optimize thermochromic houses in composites. DFT explains how electron-phonon coupling drives thermochromism through modeling how thermal vibrations affect electronic states (Ji, F. et al., 2023). DFT is also applied to analyze thermodynamic residences together with free energy changes in polymer conformational changes (Qing, L. 2024). In addition, when DFT is carried out with UV-vis spectroscopy, the fashions acquired may be confirmed, and a comprehensive elucidation on thermochromic conduct may be inferred (Ji, F. et al., 2023). Clearly, DFT studies of the binary polymer combination would probe how interactions between additives have an effect on the thermochromic reaction (Williams, M.W. et al., 2023). Lastly, DFT also studies mechanical residences to guarantee the performance of thermochromic materials in the environment they function (Zhang, W. et al., 2021).

In this study, three surfactants are incorporated; a cationic [CTAB (cetyltrimethylammonium bromide)], an anionic [SDS (sodium dodecyl sulfate)], and a nonionic surfactant [Triton X-100]. These surfactants had been decided on to cover special surfactant lessons and to analyze their various interactions with PCDA. The concept is figuring out the surfactant attention for each type to be able to maximize the color trade at decrease temperatures. To make clear a relation between the structural capabilities in PCDA-surfactant complicated and its thermochromic pastime. To this end, PCDA solutions of varying surfactant concentrations were prepared. PCDA monomers undergo polymerization upon UV initiation at a given wavelength. The thermochromic properties of the final PCDA-surfactant composites are then characterized. Characterization is performed by techniques like UV-vis spectroscopy to monitor the shift in color of the composites with respect to temperature. Quantitative measurement of color changes and calorimetric response (CR) of the materials is performed with CIE-Lab* colorimetric analysis. As surfactant type is shown to influence the size and morphology of the PCDA particles, a detailed particle size analysis is done. This aspect aids in linking the particle size to the measured thermochromic actuation. In addition, molecular interaction between PCDA and the surfactants is discussed through computational studies using Density Functional Theory (DFT). the paper presents a complete picture about how surfactants influence the thermochromic properties of PCDA.

2. EXPERIMENTAL PART

2.1. Materials

PCDA monomer (10,12-pentacosadiynoic acid), with cash number (66990-32-7) and molecular weight of 374.6 g/mol, was obtained from Shanghai Aladdin Biochemical Technology Co. Ltd., China. Three surfactant kinds were acquired, which are:

- Anionic surfactant: SDS (Sodium dodecyl sulfate), cash number (151-21-3) from Bide pharmatech Ltd., China.
- Cationic surfactant: CTBA (n,n,n-Trimethylammonium Bromide), cash number (57-09-0) from Bide pharmatech Ltd., China.
- Nonionic surfactant: Triton X-100, cash number (9036-19-5) from Dow Chemical Pacific Ltd., Middle East.

2.2. The used instruments

The following are the used instruments in this study:

- The sonication process was performed with a cyclon sonicator type SJIA-1200W Ultrasonic cell crusher (Ningbo Sklon Lab Instrument Co., Ltd., China).
- Polymerization process was carried out using a UV-Vis lamp Polish-made Naswielacz UV 245 wavelength 256 nm.
- The size distribution of the DLS 9900 nanoparticle size analyzer (K-One Nano Ltd., Seoul, Korea) was used to determine the particle size.
- The UV spectra were obtained using a UV-1800 spectrometer (Shimadzu Crop., Kyoto, Japan).
- Chromatic features of CIE-Lab are obtained using a Datacolor model DC10-2 CIE-Lab device ColorReader.

2.3. Preparation and Characterization Methods

The procedure to preparation samples from PCDA monomer + surfactant following steps:

- Solved 0.015 g from PCDA monomer by using 15 ml chloroform in beaker (100 ml size).
- Leave the solution until the chloroform evaporates and forms a thin layer of PCDA at the bottom of the beaker.
- Then add surfactant as shown in table 1. into the beaker to preparation samples PCDA/surfactant.
- The beaker was then filled with 40ml of distilled water (DW) and sonicated for ten minutes.
- The procedure was then repeated after an additional 20 mL of DW was added and sonicated for five minutes. Until the desorption sonication period was 20 minutes, and the total volume of the solution was 80 ml.

- Then the sonicated vesicle solution was kept in a refrigerator at 4°C for 24 hours.
- The vesicle solution was exposed to 254 nm UV light in order to polymerize it. Ultimately, a PCDA and surfactant-based mixed vesicle solution was created.

Table 1. The amount for surfactants in samples PCDA/ surfactant

PCDA/ SDS		PCDA/CTBA		PCDA/Triton (X-100)	
Sample No.	SDS (g)	Sample No.	CTBA (g)	SampleNo.	Triton (X-100) (ml)
1	0.003	1	0.003	1	0.5
2	0.006	2	0.006	2	1
3	0.009	3	0.009	3	1.5
4	0.012	4	0.012	4	2
5	0.015	5	0.015	5	2.5

2.4. Chromatic properties of CIE-Lab

Color shifting is provided by the CIE-Lab* device when materials are subjected to temperature changes. The L*, a*, and b* parameters are used to represent these shifts; L* stands for lightness, a* for the green-red axis, and b* for the blue-yellow axis. At a baseline temperature, this apparatus records the material's original color. A collection of L*, a*, and b* values are used to record this. The device then records any changes in the L*, a*, and b* values while measuring the color once more at predefined intervals and as the temperature is gradually changed. Finally, to ascertain the colorimetric response (CR or ΔE), the initial and subsequent measurements were compared using the following formula (Arruda, B.M., et al., 2021):

$$CR = \Delta E = \sqrt{\Delta L^2 + \Delta a^2 + \Delta b^2} \quad (1)$$

High CR values indicate a strong and discernible color change with temperature changes, which is ideal for some applications where temperature changes must be immediately recognized and clear visual cues are required. Temperature indicators, safety indicators, and smart packaging are some of these uses. On the other hand, textile applications that favor gradual color changes are better served by low CR values.

3. RESULTS AND DISCUSSION

3.1. The Change Color for vesicle system with temperature

In the current work, three surfactant types were applied to expand the interval play span of PCDA polymer below 60 °C. The surfactant content was regulated as shown in Table 1. Fig. 1 displays the outcomes for vesicles made with PCDA and surfactant. According to the results, for the majority of surfactant ratios, PCDA/surfactant colors shifted from blue to red below 40 °C. Because of these early color changes, PCDA polymer will be able to be utilized as a body-temperature strip monitor throughout a larger temperature range, down to 36°C. These flexible strips are often used by doctors to take their patient's temperatures. These strips typically have a sensitivity range of 36 to 40 degrees Celsius. Additionally, Fig. 1. yields the following results:

1. For PCDA/SDS vesicles, the color does not change at low ratios and begins to change starting from 0.006 g SDS.
2. For PCDA/CTBA vesicles, the color changed gradually with CTBA amounts.
3. For PCDA/Triton X-100 vesicles, the color changed at low ratios only and then be stable.
4. The best changes occurred with 0.012g SDS, 0.015g CTBA and 1 ml Triton X-100.

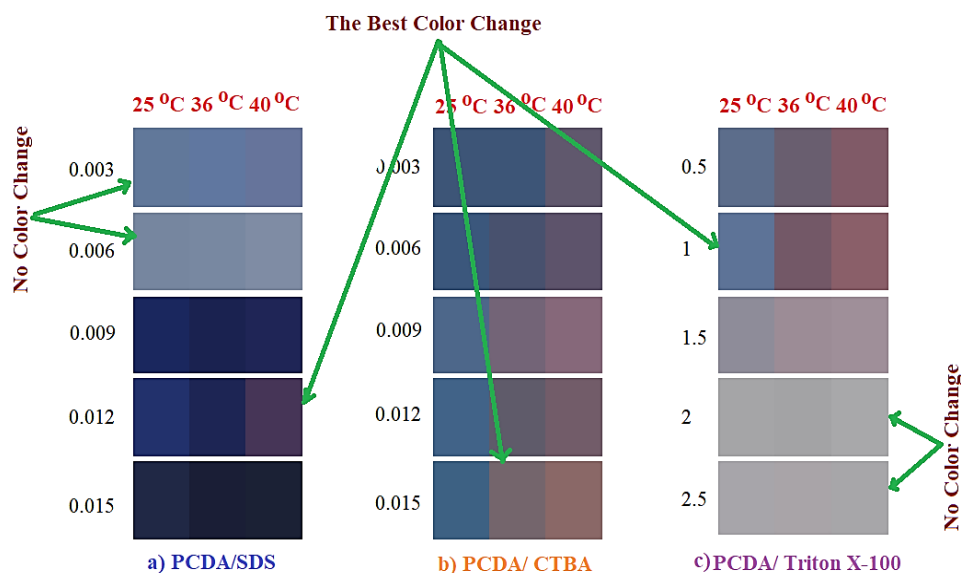


Fig. 1. Effect of surfactant types and amounts on the colour change of PCDA vesicles

Therefore, these best samples will be studied further from the viewpoints of UV absorbance Fig. 2, calorimetric response (CR or ΔE) by C.I.E Lab device Table 2 and particle size analyzing Fig. 3 to Fig. 5 and Table 3.

3.2. UV absorbance results

The absorbance of the above three best surfactant ratios was tested by UV spectra to illustrate reasons behind these colors changing Fig. 2. It is clear that all samples have two maximum absorbance wavelengths, around 640 nm and around 540 nm. The intensities of these absorbances decreased as temperature increased, and as the color went toward red, the maximum absorbance position shifted upward (İlkiz, B.A. et al., 2021; Mohammed, M. et al., 2019).

3.3. CIE-Lab* properties analysis

Table 2. shows the color coordinate values of the standards (at room temperature; 25°C) for the three best samples compared with samples at 36°C and 40°C. The results show conclusively that the color change for vesicles of PCDA with all three surfactants exhibits a clear temperature dependence of blue throat (40°C) to red (60°C) transition. This change is supported also through the ΔE values (Table 2), showing high values at 40°C compared to 36°C, thus confirming the UV spectra results. CTBA showed the largest color difference ($\Delta E = 33.73$

at 40°C), followed by Triton X-100 ($\Delta E = 29.55$) and SDS ($\Delta E = 18.88$), indicating that the presence of surfactants varies the sensitivity of vesicles to temperature changes (Kim, J. et al., 2021; Hakami, A. et al., 2022). This strongly suggests that CTBA is the main driver for the thermochromic properties of the PCDA vesicles.

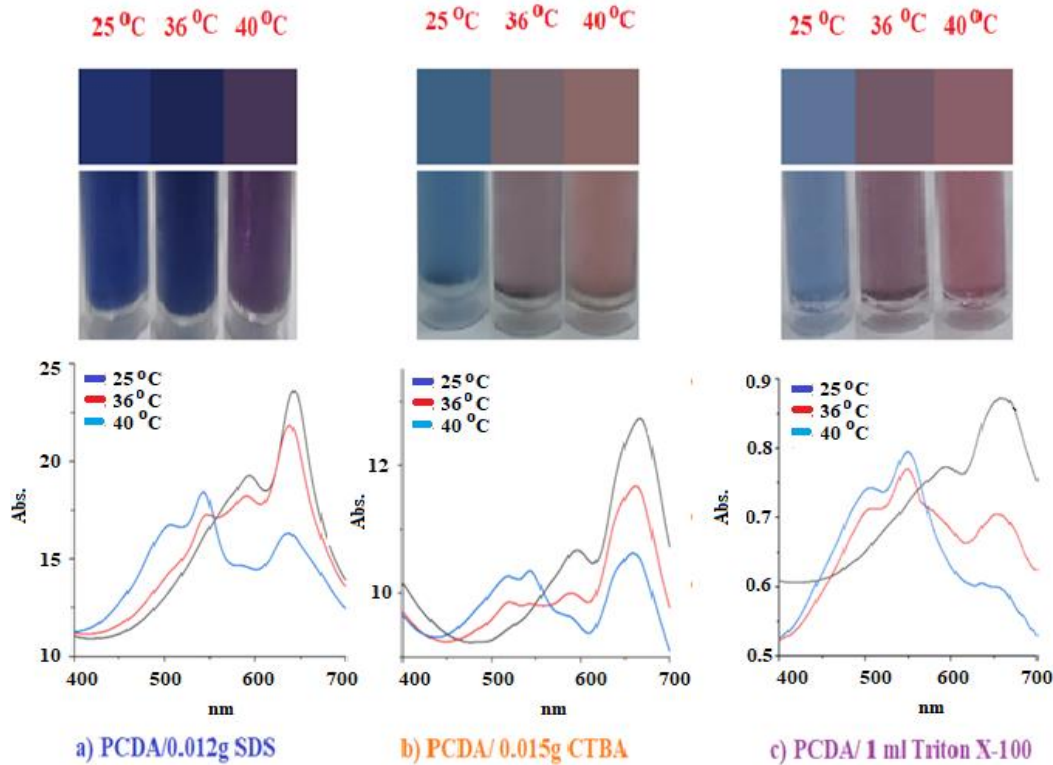


Fig. 2. Color changes and UV-absorbance of the best surfactant ratios at different temperatures

Table 2. C.I.E. L*a*b* data sets for the best three vesicles at 25oC, 36oC and 40oC.

PCDA / 0.012 g SDS vesicle: L= 22.37, a=15.01, b=-36.324							
Temp.	L	a	b	ΔL	Δa	Δb	$\Delta E = \sqrt{\Delta L^2 + \Delta a^2 + \Delta b^2}$
36°C	16.622	13.217	-29.795	-5.748	-1.793	6.529	8.88
40°C	25.371	15.292	-17.686	3.001	0.282	18.638	18.88
PCDA / 0.015 g CTBA vesicle: L= 39.881, a=-2.529, b=-22.909							
36°C	44.381	7.287	-1.741	4.5	9.816	21.168	23.76
40°C	47.345	13.454	5.851	7.464	15.983	28.76	33.73
PCDA / 0.015 g CTBA vesicle: L= 39.881, a=-2.529, b=-22.909							
36°C	40.58	13.79	-4.308	-7.455	12.415	17.791	22.93
40°C	45.093	19.06	1.402	-2.942	17.685	23.501	29.55

3.4. Particle size analysis

The effects of temperature on the particle sizes of PCDA containing different surfactants (0.015g CTBA or 1 ml Triton or 0.012g SDS) were shown in Fig. 3. to Fig. 5. respectively, while Table 3. summarizes these results. For PCDA containing SDS surfactant, the D50 parameter decreased from 566.9 to 1.706 μm , while the SSA increased from 6.009 to 441.3 m^2/kg .

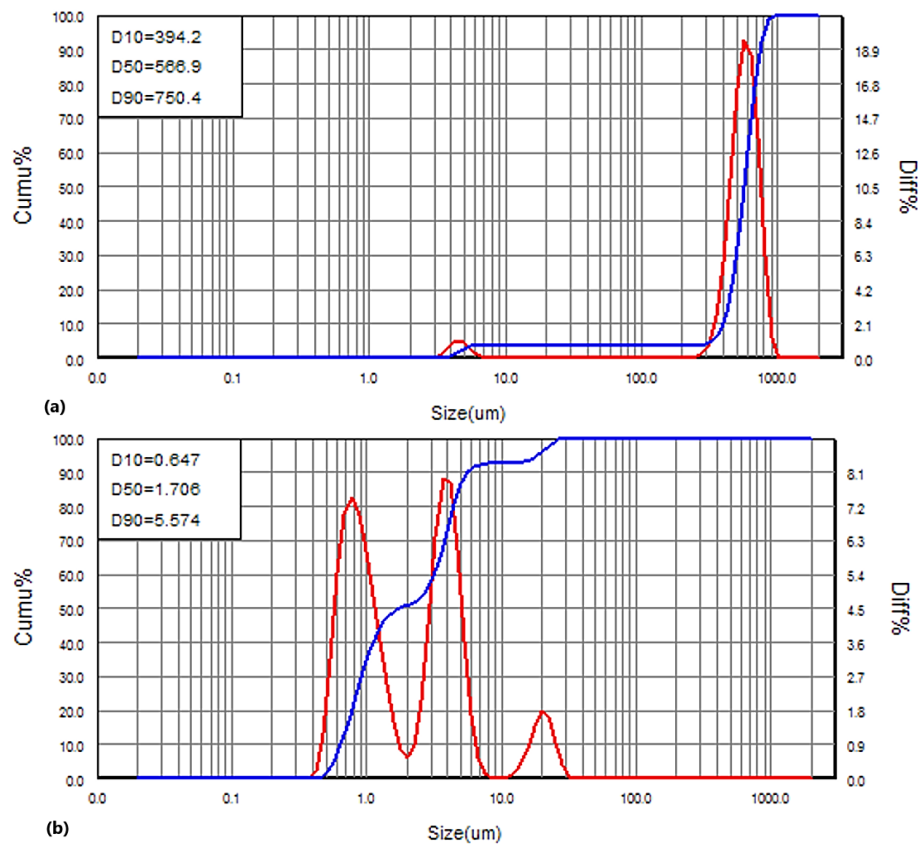


Fig. 3: Distribution of particle sizes for PCDA containing SDS surfactant at a) 25°C and b) 40°C

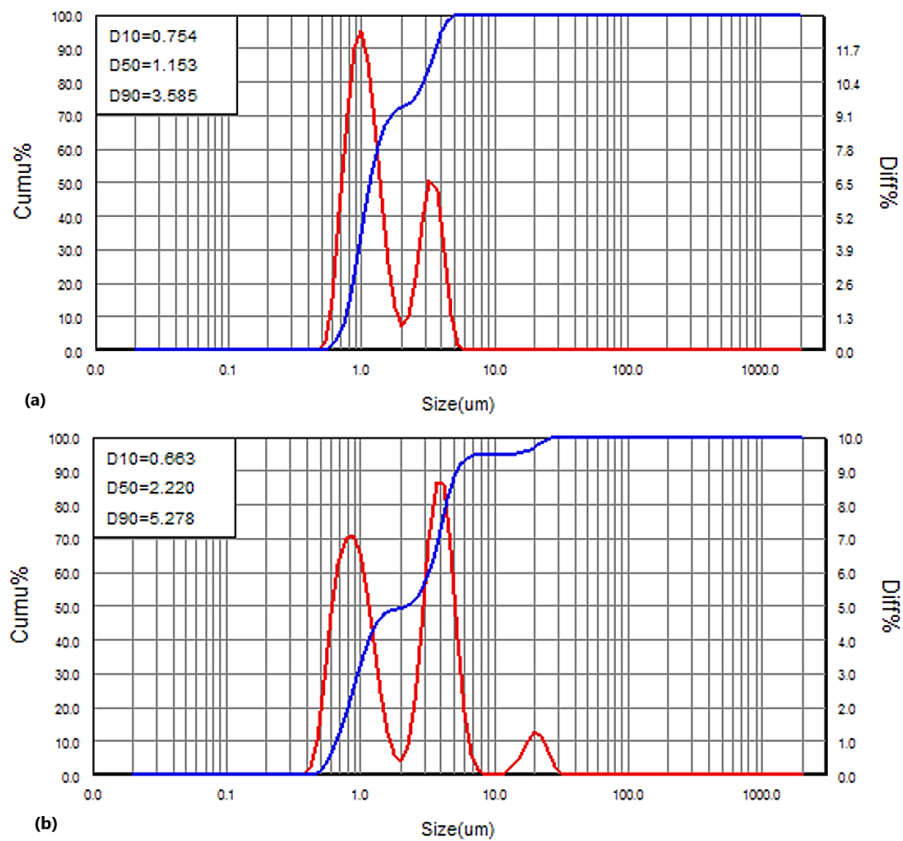


Fig. 4: Distribution of particle sizes for PCDA containing CTBA surfactant at a) 25°C and b) 40°C.

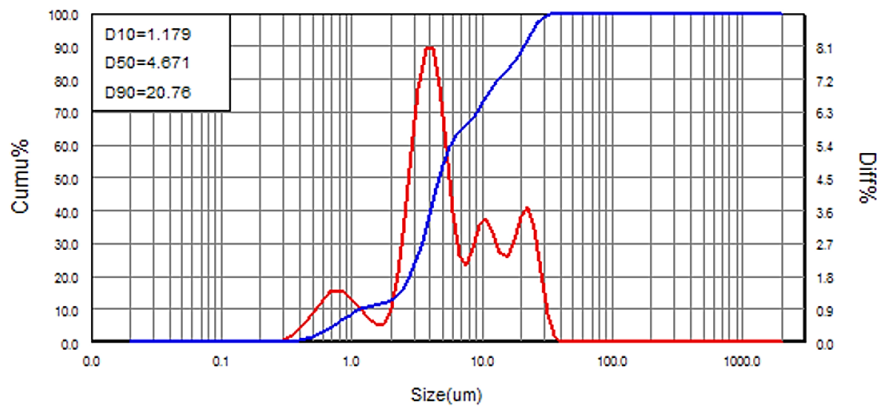


Fig. 5: Distribution of particle sizes for PCDA containing 1 wt.% Triton surfactant at 25°C

It is clear that the particle size of Triton surfactant is larger than the CTBA surfactant due to the following reasons:

1. Triton, is a nonionic surfactant, forms micelles with a relatively larger hydrodynamic diameter compared to the smaller, more compact micelles formed by the cationic CTAB.
2. The larger Triton micelles have a greater capacity to solubilize and encapsulate hydrophobic compounds within their core, leading to the formation of larger micellar structures. CTAB, with its smaller micelle size, has a lower solubilization capacity for hydrophobic species compared to Triton.

Table 3. D10, D50, D90 and SSA for the used surfactants at 25°C and at 40°C.

Surfactant Amount and Type	Temperature (°C)							
	25°C				40°C			
	D10 (μm)	D50 (μm)	D90 (μm)	SSA (m^2/kg)	D10 (μm)	D50 (μm)	D90 (μm)	SSA (m^2/kg)
0.012g (SDS)	394.2	566.9	750.4	6.009	0.674	1.706	5.574	441.3
0.015g (CTBA)	0.754	1.153	3.585	494.9	0.663	2.220	5.278	429.9
1 ml Triton X-100	1.179	4.671	20.76	198.7	The particle size has disappeared			

3. The positive charge of CTAB allows it to interact with and bind to negatively charged species, such as DNA or proteins, leading to the formation of larger charged complexes. Triton, being nonionic, does not participate in these types of charge-driven interactions, and therefore does not typically form larger charged complexes.

4. When comparing SDS surfactant with the both CTBA and Triton surfactants, it's clear that SDS form the largest particle sizes with the PCDA polymer, where the D50 is 566.9 μm for SDS compared with 1.153 μm and 4.671 μm for CTBA and Triton respectively.

This is belonging to the following reasons:

- a. The electrostatic interactions between the neutral PCDA polymer and the negatively charged SDS are weaker than those between PCDA and the cationic CTAB or Triton. These weak interactions resulted in the formation of larger surfactant-PCDA aggregates or particles, as the surfactant molecules are less constrained in their packing and organization within the PCDA

matrix. The strength of these interactions can affect the degree of surfactant incorporation within the PCDA matrix.

b. On the other hand, the longer hydrophobic tail of SDS (12 carbon atom) leads to stronger hydrophobic interactions with the PCDA polymeric chains, which resulted in the formation of larger surfactant-PCDA aggregates or particles (Herez, M.H. et al. 2023). This high D50 value for SDS surfactant agrees with its low CR value and low SSA value.

From the viewpoint of temperature effects, the D50 of PCDA containing CTAB increased from 1.153 μm at RT to 2.220 μm at 40°C due to the hydrophobic interactions among the long alkyl chains of CTAB molecules become stronger, which resulting in formation of larger micellar structures (Das, S. et al. 2020). The particle size of Triton-based systems may change with temperature due to changes in micelle size and solubilization capacity. Sodium dodecyl sulfate (SDS) is an anionic surfactant and has the following structure: $\text{CH}_3\text{-(CH}_2\text{)}_{11}\text{-O-SO}_3\text{-Na}^+$. That means, SDS has amphiphilic nature because it contains both hydrophobic alkyl chain (12 carbon atoms) and a hydrophilic, negatively charged (polar) sulfate head group. This dual nature enables SDS to form micelles in aqueous solutions above its critical micelle concentration (CMC) (Figueiredo, M.T.D. et al., 2024). For all these reasons, the D50 of SDS/PCDA system decreased largely from 566.9 μm to 1.706 μm (as the temperature increased from RT to 40°C) as well as the SSA increased from 6.009 to 441.3 m^2/kg . This high increment in the SSA means that SDS/PCDA thermochromic system can provide rapid and sensitive temperature detection, enabling their use in temperature indicators (e.g., for food, beverages, and consumer products) as well as in temperature monitoring in industrial and medical applications.

3.5. Optimized and Electronic structures of polymeric composites

In this part of the work, the polymeric composites PCDA, PCDA/SDS, PCDA/CTBA, and PCDA/Triton X-100 were designed and prepared using GaussView 6.0.16, as shown in Fig. 6. While these calculations involved the use of the density functional theory B3LYP/DFT functional model and the basis set 6-311G(d,p) by the Gaussian 09 software package, to ensure and measure all geometrical features accurately. The geometric optimization analysis of PCDA and grafted polymeric additives confirmed that the optimized structures are in good agreement with the experimental data and thus there is agreement on the computational technique used in this work, which is the density function theory, to provide the geometric properties of polymer systems to obtain good regularity and arrangement of the additives with the polymer network and thus physical and chemical compatibility of the optimized composites, as shown in Fig. 6. Table 4. Presents the effects of the floor country calculations finished on the polymeric composites in this take a look at, with a selected attention on identifying the energy-minimizing

configurations. These calculations encompass a set of parameters, such as overall strength (ET), ionization potential (IP), and electron affinity (EA). Furthermore, the strength gap (Eg), which represents the power difference among the very best occupied molecular orbital (HOMO) and the bottom unoccupied molecular orbital (LUMO), is calculated. Eg serves as a degree of the conductivity of the fabric and presents insights into its potential for electronic and thermal packages (Abud, S.H. et al., 2021). The general energy (ET) of the polymeric composites investigated in this study shows a massive increase with the inclusion of Sodium dodecyl sulfate, Trimethylammonium Bromide and Triton X-a 100 in comparison to natural PCDA.

This commentary suggests that the presence of delivered molecules in the composite machine leads to an improved total electricity country. The introduction of those debris into the PCDA matrix initiates extra intermolecular interactions and forces and for that reason engages in electrostatic interactions with the surrounding molecules in the composite gadget which in turn are encouraged by the prices gift at the particles and the surrounding molecules (Jebur, S.K. et al., 2022).

In addition to the presence of hydrogen bonding between the functional groups on the added particles and the polymer matrix, this type of interaction also contributes to the stability and alignment of the particles within the composite. All of this together contributes to increasing the overall energy of the composite system, and it is worth noting that this confinement requires energy input associated with the breaking of bonds or forces within the PCDA matrix, which favors the dispersion or alignment of the particles, thereby increasing the overall energy of the system (Hasan, A.S. et al., 2022). Comparing the data in Table 2, it is clear that the polymer compounds examined have higher ionization potential (IP) and electron affinity (EA) values compared to pure PCDA. A higher IP indicates a greater tendency for the material to retain electrons, while a higher EA indicates an enhanced ability to attract additional electrons. These differences in electronic properties between the compounds can be attributed to a variety of factors, including changes in chemical composition, structure, and bonding characteristics (AL-Abass, S.F.A. et al., 2023). The incorporation of SDS, CTBA, and Triton X-100 into the PCDA matrix introduces additional functional groups that can donate or accept electrons, thus changing the overall electronic behavior of the compound. This modification of the electronic properties is influenced by changes in the chemical environment, such as different bond configurations. The introduction of these elements results in the inclusion of electron donor or electron acceptor groups, thus changing the overall electronic behavior of the compound (Hassan, H.B. et al., 2024 and Weston, M. et al., 2020). The higher IP and EA values observed in the doped polymer composites compared to pure PCDA can also be attributed to the

introduction of additional SDS, CTBA, and Triton X-100 electron donor or acceptor groups (Khanantong, C. et al., 2019). These changes in electronic behavior have an impact on the performance of the composites in various applications, especially electronic devices or heat-related systems (Feng, Y.Q. et al., 2022). Table 2 shows the energy levels of the highest occupied molecular orbital (HOMO) and the lowest unoccupied molecular orbital (LUMO) for the pure and doped PCDA structures. These results indicate a more stable electron distribution compared to PCDA alone. This increased stability can be attributed to the electron-withdrawing properties of the SDS, CTBA and Triton X-100 materials, which indicate a stronger tendency to attract and accept electrons (Ortega, P.F. et al., 2021). When incorporated into the polymer matrix, the additives act as electron acceptors, leading to a redistribution of the electron density within the system. By pulling electrons from the surrounding PCDA molecules. Through these results, we observe a decrease in the energy gap values, despite being high. This confirms that the materials examined are close to the semiconductor range and therefore have a thermal resistance with a negative thermal coefficient, i.e., α . As the conductivity increases, the thermal value decreases. This is confirmed by the actual results obtained, so they can be used as colored thermal materials due to their ability to change color in response to temperature changes. B. The thermal materials are integrated into windows to regulate sunlight and heat transfer according to temperature changes, improving energy efficiency and increasing the comfort of buildings. In addition, their applications are also used in indicators or temperature-sensitive sensors to visually display temperature changes in various systems and environments. They are also used in medical devices for temperature monitoring, wound healing applications, or as indicators for temperature-sensitive medical products (Wu, L. et al., 2021 and Hasan, A.S. et al., 2024).

Table 4. Calculated Electronic Properties of polymeric composites Using the B3LYP/DFT Level of Theory

Samples	ET	HOMO	LUMO	Eg	IP	EA
PCDA	-9632.24	-11.4370	-7.5317	3.905	11.437	7.532
PCDA/SDS	-8531.38	-11.2364	-7.4322	3.804	11.236	7.432
PCDA/CTBA	-8376.34	-11.0358	-7.2786	3.757	11.036	7.279
PCDA/Triton X-100	-8037.98	-10.8352	-7.1234	3.712	10.835	7.123

This commentary suggests that the presence of delivered molecules in the composite machine leads to an improved total electricity country. The introduction of those debris into the PCDA matrix initiates extra intermolecular interactions and forces and for that reason engages in electrostatic interactions with the surrounding molecules in the composite gadget which in turn are encouraged by the prices gift at the particles and the surrounding molecules (Jebur, S.K. et al., 2022).

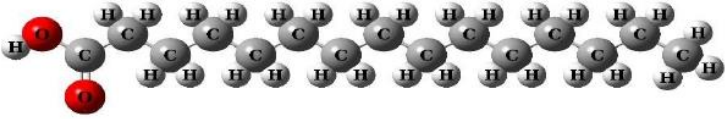
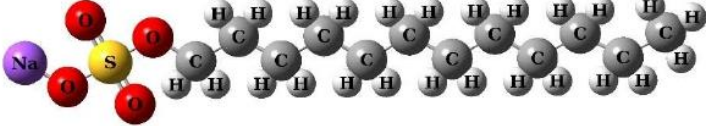


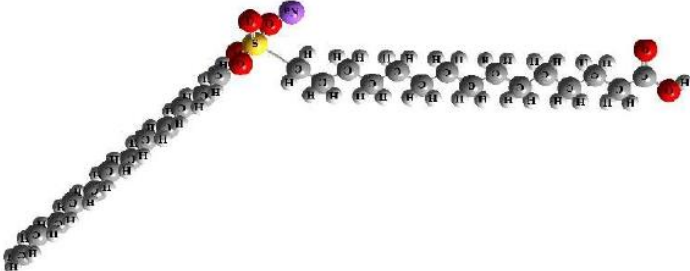
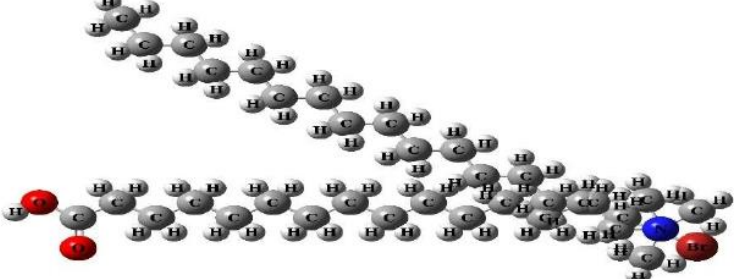
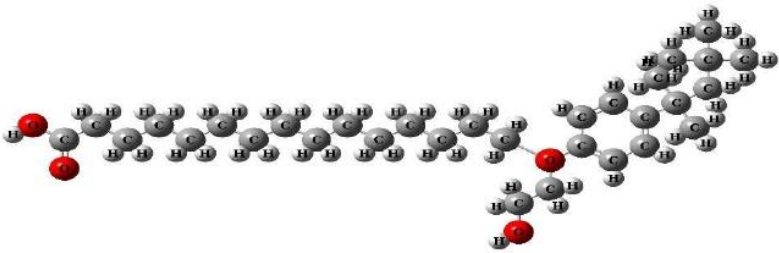
Sample	Structural
Polydiacetylene (PCDA)	
Sodium dodecyl sulfate (SDS)	
Trimethylammonium Bromide (CTBA)	
Triton X-100	
PCDA/SDS	
PCDA/CTBA	
PCDA/Triton X-100	

Fig. 6. Optimized molecular structures of polymeric composites Using the B3LYP/DFT Level of Theory.

In addition to the presence of hydrogen bonding between the functional groups on the added particles and the polymer matrix, this type of interaction also contributes to the stability and alignment of the particles within the composite. All of this together contributes to increasing the overall energy of the composite system, and it is worth noting that this confinement requires energy input associated with the breaking of bonds or forces within the PCDA matrix, which favors the dispersion or alignment of the particles, thereby increasing the overall energy of the system (Hasan, A.S. et al., 2022). Comparing the data in Table 2, it is clear that the polymer compounds examined have higher ionization potential (IP) and electron affinity (EA) values compared to pure PCDA. A higher IP indicates a greater tendency for the material to retain electrons, while a higher EA indicates an enhanced ability to attract additional electrons. These differences in electronic properties between the compounds can be attributed to a variety of factors, including changes in chemical composition, structure, and bonding characteristics (AL-Abass, S.F.A. et al., 2023). The incorporation of SDS, CTBA, and Triton X-100 into the PCDA matrix introduces additional functional groups that can donate or accept electrons, thus changing the overall electronic behavior of the compound. This modification of the electronic properties is influenced by changes in the chemical environment, such as different bond configurations. The introduction of these elements results in the inclusion of electron donor or electron acceptor groups, thus changing the overall electronic behavior of the compound (Hassan, H.B. et al., 2024 and Weston, M. et al., 2020). The higher IP and EA values observed in the doped polymer composites compared to pure PCDA can also be attributed to the introduction of additional SDS, CTBA, and Triton X-100 electron donor or acceptor groups (Khanantong, C. et al., 2019). These changes in electronic behavior have an impact on the performance of the composites in various applications, especially electronic devices or heat-related systems (Feng, Y.Q. et al., 2022). Table 2 shows the energy levels of the highest occupied molecular orbital (HOMO) and the lowest unoccupied molecular orbital (LUMO) for the pure and doped PCDA structures. These results indicate a more stable electron distribution compared to PCDA alone. This increased stability can be attributed to the electron-withdrawing properties of the SDS, CTBA and Triton X-100 materials, which indicate a stronger tendency to attract and accept electrons (Ortega, P.F. et al., 2021). When incorporated into the polymer matrix, the additives act as electron acceptors, leading to a redistribution of the electron density within the system. By pulling electrons from the surrounding PCDA molecules. Through these results, we observe a decrease in the energy gap values, despite being high. This confirms that the materials examined are close to the semiconductor range and therefore have a thermal resistance with a negative thermal coefficient, i.e., $\alpha < 0$. As the conductivity increases, the thermal

value decreases. This is confirmed by the actual results obtained, so they can be used as colored thermal materials due to their ability to change color in response to temperature changes. B. The thermal materials are integrated into windows to regulate sunlight and heat transfer according to temperature changes, improving energy efficiency and increasing the comfort of buildings. In addition, their applications are also used in indicators or temperature-sensitive sensors to visually display temperature changes in various systems and environments. They are also used in medical devices for temperature monitoring, wound healing applications, or as indicators for temperature-sensitive medical products (Wu, L. et al., 2021 and Hasan, A.S. et al., 2024).

4. CONCLUSIONS

PCDA interval play temperature can be broaden down to 36oC instead of 60oC by using the suitable amount and type of surfactant. This expanded span temperature enables PCDA polymer to be utilized as flexible strips for a body-temperature monitor, which often used by doctors to take their patients' temperatures. For the used surfactants, there is some fluctuations in color changes with the used ratios and the best changes occurred with 0.012g SDS, 0.015g CTBA and 1 ml Triton X-100. As temperature increased, the absorbance intensities decreased and the color going toward the red. Based on calorimetric response (CR) results, PCDA polymer can be used in wide applications spectrum (from textile uses to safety indicators and smart packaging) according to the used surfactant. The particle size shows variations with the surfactant type, temperature and therefore the intended application. The main results of electronic simulations using density functional theory (DFT) with the B3LYP functional model and the 6-311G(d,p) basis set are represented by the help of electronic simulations using density functional theory (DFT) with the B3LYP functional model and the 6-311G(d,p) basis set in optimizing the structures of polymeric compounds such as PCDA, PCDA/SDS, PCDA/CTBA, and PCDA/Triton X-100, ensuring that the calculated structures are in good agreement with the experimental data. Electronic simulations using DFT also allowed the calculation of various electronic properties, including total energy (ET), ionization potential (IP), electron affinity (EA), energy gap (Eg), highest occupied molecular orbital (HOMO), and lowest unoccupied molecular orbital (LUMO) of the polymeric compounds under study. The calculations focused on determining the energy-minimizing configurations of the polymeric compounds. Parameters such as total energy (ET), ionization potential (IP), electron affinity (EA), and energy gap (Eg) were determined to provide insights into the electronic behavior and stability of the compounds. The results showed that polymeric compounds with additives such as sodium dodecyl sulfate,

trimethylammonium bromide, and Triton X-100 exhibited higher values of ionization potential (IP) and electron affinity (EA) compared to pure PCDA. This indicates changes in the electronic properties of the compounds due to the introduction of additional electron donor or acceptor groups. The analysis of the HOMO and LUMO energy levels, along with the energy gap values, indicates that the studied materials are close to being in the semiconductor field. This suggests potential applications in thermoelectric materials with color-changing properties based on temperature changes, energy-efficient building materials, temperature-sensitive sensors, and medical devices for temperature monitoring and wound healing. In summary, the electronic simulation results using DFT with the B3LYP functional model and the 6-311G(d,p) basis set provided valuable insights into the optimized structures, geometric properties and electronic behavior of polymeric compounds, providing a comprehensive understanding of their molecular-level properties and potential applications.

5. REFERENCES

Abud, S.H., Hasan, A.S., Almaamori, M. and Bayan, N., 2021, March. Enhancement the ability to pump crude oil using rubber solutions. In *Journal of Physics: Conference Series* (Vol. 1818, No. 1, p. 012235). IOP Publishing.

AL-Abass, S.F.A., Braihi, A.J. and Hasan, A., 2023, September. Oil spill cleaning up by polymeric sorbents using salt leaching method. In *AIP Conference Proceedings* (Vol. 2839, No. 1). AIP Publishing.

Arruda, B.M., Bassi, J.C., Vitti, R.P. and Scatolin, R.S., 2021. Color stability of bulk fill composite resins submitted to coffee staining. *Brazilian Dental Science*, 24(1), pp.7-p.

Banjar, M.F., Joynal Abedin, F.N., Fizal, A.N.S., Muhamad Sarih, N., Hossain, M.S., Osman, H., Khalil, N.A., Ahmad Yahaya, A.N. and Zulkifli, M., 2023. Synthesis and Characterization of a Novel Nanosized Polyaniline. *Polymers*, 15(23), p.4565.

Crosby, P.H. and Netravali, A.N., 2022. Green thermochromic materials: a brief review. *Advanced Sustainable Systems*, 6(9), p.2200208.

Das, S., Lazenby, R.A., Yuan, Z., White, R.J. and Park, Y.C., 2020. Effect of laser irradiation on reversibility and drug release of light-activatable drug-encapsulated liposomes. *Langmuir*, 36(13), pp.3573-3582.

Feng, Y.Q., Lv, M.L., Yang, M., Ma, W.X., Zhang, G., Yu, Y.Z., Wu, Y.Q., Li, H.B., Liu, D.Z. and Yang, Y.S., 2022. Application of new energy thermochromic composite thermosensitive materials of smart windows in recent years. *Molecules*, 27(5), p.1638.

- Figueiredo, M.T.D., Neves, H.P., Mageste, A.B., Patiño-Agudelo, A.J., Ferreira, G.M.D. and Ferreira, G.M.D., 2024. Liquid–Liquid Equilibrium of Aqueous Two-Phase Systems Formed by Nonionic Surfactants (Triton X-100, Triton X-165, or Triton X-305), Salts (NaNO₃ or KNO₃), and Water at Different Temperatures. *Journal of Chemical & Engineering Data*, 69(3), pp.1159-1168.
- Gupta, S., Chatterjee, S., Zolnierczuk, P., Nesterov, E.E. and Schneider, G.J., 2020. Impact of local stiffness on entropy driven microscopic dynamics of polythiophene. *Scientific reports*, 10(1), p.9966.
- Hakami, A., Biswas, P.K., Emirov, Y., Stefanakos, E.K. and Srinivasan, S.S., 2022. Effect of surfactant on the TiO₂ microencapsulation of Thermochromic materials. *International Journal of Energy Research*, 46(8), pp.10590-10605.
- Hasan, A.S., Hassan, H.B., Hashim, A., Hasan, N.B. and Al-kawaz, Y.A., 2024. Modeling, Fabrication and Characteristics of Novel (PVA-SiC-In₂O₃) Nanohybrid Structures for Optoelectronic Applications. *Silicon*, pp.1-14.
- Hasan, A.S., Mousa, A.H. and Hussein, A.R.A., 2022, March. Molecular Dynamics Simulation of SWCNT/PYA in sensors application. In 2022 Muthanna International Conference on Engineering Science and Technology (MICEST) (pp. 83-88). IEEE.
- Hassan, H.B., Hasan, A.S. and Hashim, A., 2024. Fabrication and advanced optical and electronic characteristics of PVA/SiC/CeO₂ hybrid nanostructures for augmented nanoelectronics and optics fields. *Optical and Quantum Electronics*, 56(3), p.309.
- Herez, M.H., Al Nageim, H., Richardson, J. and Wright, S., 2023. DEVELOPMENT OF A PREMIUM COLD MIX ASPHALT. *Kufa Journal of Engineering*, 14(3), pp.30-47.
- Hossain, M.I., Khan, M.S., Khan, I.K., Hossain, K.R., He, Y. and Wang, X., 2024. TECHNOLOGY OF ADDITIVE MANUFACTURING: A COMPREHENSIVE REVIEW. *Kufa Journal of Engineering*, 15(1), pp.108-146.
- Hossain, S., Sadoh, A. and Ravindra, N.M., 2022. Principles, properties and preparation of thermochromic materials.
- Ibadat, N.F., Ongkudon, C.M., Saallah, S. and Misson, M., 2021. Synthesis and characterization of polymeric microspheres template for a homogeneous and porous monolith. *Polymers*, 13(21), p.3639.

İlkiz, B.A., Beceren, Y.İ. and Candan, C., 2021. An approach to estimate dye concentration of domestic washing machine wastewater. *Autex Research Journal*, 21(2), pp.172-181.

Jebur, S.K., Braihi, A.J. and Hassan, A.S., 2022. Graphene effects on the structural, morphological and optical properties of PEDOT: PSS thin films. *Materials Today: Proceedings*, 49, pp.2733-2740.

Ji, F., Klarbring, J., Zhang, B., Wang, F., Wang, L., Miao, X., Ning, W., Zhang, M., Cai, X., Bakhit, B. and Magnuson, M., 2023. Remarkable Thermochromism in the Double Perovskite Cs.

Khanantong, C., Charoenthai, N., Kielar, F., Traiphol, N. and Traiphol, R., 2019. Influences of bulky aromatic head group on morphology, structure and color-transition behaviors of polydiacetylene assemblies upon exposure to thermal and chemical stimuli. *Colloids and Surfaces A: Physicochemical and Engineering Aspects*, 561, pp.226-235.

Kim, J., Yun, H., Lee, Y.J., Lee, J., Kim, S.H., Ku, K.H. and Kim, B.J., 2021. Photoswitchable surfactant-driven reversible shape-and color-changing block copolymer particles. *Journal of the American Chemical Society*, 143(33), pp.13333-13341.

Kim, I.J., Manivannan, R. and Son, Y.A., 2018. Thermally reversible Fluorans: Synthesis, Thermochromic properties and real time application. *Journal of nanoscience and nanotechnology*, 18(5), pp.3299-3305.

Mohammed, M., Diwan, A., Saleh, S.M. and Salih, B.A.S., 2019. Fabrication of copper nanoparticles by pulse laser ablation. *Kufa Journal of Engineering*, 10(1), pp.1-11.

Ortega, P.F., Galvão, B.R., de Oliveira, P.S., Bastos, G.A., Bernardes, M.R., Lavall, R.L. and Trigueiro, J.P., 2021. Thermochromism in Polydiacetylene/Poly (vinyl alcohol) Hydrogels Obtained by the Freeze–Thaw Method: A Theoretical and Experimental Study. *Industrial & Engineering Chemistry Research*, 60(36), pp.13243-13252.

Qing, L., Wang, X., Li, S., Zhang, J. and Jiang, J., 2024. Thermodynamic Perturbation Theory for Charged Branched Polymers. *Journal of Chemical Theory and Computation*, 21(1), pp.333-346.

Stanfield, M.K., Weerts, C.A., Timilsina, M.P., Smith, J. and Thickett, S.C., 2024. Bioderived Thiol–Ene Emulsion Polymerization for Hybrid Latex Particles. *Biomacromolecules*, 25(10), pp.6580-6590.

- Wang, Y.Y., Guo, F.L., Li, Y.Q., Zhu, W.B., Li, Y., Huang, P., Hu, N. and Fu, S.Y., 2022. High overall performance transparent bamboo composite via a lignin-modification strategy. *Composites Part B: Engineering*, 235, p.109798.
- Weston, M., Tjandra, A.D. and Chandrawati, R., 2020. Tuning chromatic response, sensitivity, and specificity of polydiacetylene-based sensors. *Polymer Chemistry*, 11(2), pp.166-183.
- Williams, M.W., Wimberly, J.A., Stwodah, R.M., Nguyen, J., D'Angelo, P.A. and Tang, C., 2023. Temperature-Responsive Structurally Colored Fibers via Blend Electrospinning. *ACS Applied Polymer Materials*, 5(4), pp.3065-3078.
- Wu, L., Liu, Z., Guan, Y., Cui, K., Jian, M., Qin, Y., Li, Y., Yang, F. and Yang, T., 2021. Visual presentation for monitoring layer-wise curing quality in DLP 3D printing. *Rapid Prototyping Journal*, 27(10), pp.1776-1790.
- Yadav, S.N., Rai, S., Shah, P., Roy, N. and Bhattarai, A., 2022. Spectrophotometric and conductometric studies on the interaction of surfactant with polyelectrolyte in the presence of dye in aqueous medium. *Journal of Molecular Liquids*, 355, p.118949.
- Zhang, L., Jerri, H.A. and Bevan, M.A., 2023. Colloidal Deposition by Polymer-Surfactant Complexes with Dilution and Shear. *Langmuir*, 39(25), pp.8680-8689.
- Zhang, W., Yang, X., Lin, C., Feng, J., Wang, H. and Yan, W., 2021. Insight into the effect of surfactant modification on the versatile adsorption of titanate-based materials for cationic and anionic contaminants. *Chemosphere*, 269, p.129383.